Analyzing the Urban Heat Island: comprehensive methodology for data gathering and optimal design of mobile transects

Laura Romero Rodríguez [a], José Sánchez Ramos [b], Francisco José Sánchez de la Flor [b],

Servando Álvarez Domínguez [a]

a Grupo de Termotecnia, Escuela Superior de Ingenieros, University of Seville, Spain.
b Escuela Superior de Ingeniería, Departamento de Máquinas y Motores Térmicos, University of Cádiz, Spain.

Abstract

The Urban Heat Island phenomenon is an increasingly important global issue. Understanding the physical characteristics of cities is critical, which is why many studies based on mobile measurements are currently being developed. However, it is highly challenging to compare them due to the various methods that are employed. Therefore, the present work aims to propose an easily replicable methodology for achieving accurate UHI assessments in potentially any city of the world. This is done by finding a representative mobile transect through experimental data, as opposed to previous studies which select routes with a variety of land covers, with the consequent risk of overlooking the truly representative areas. The main urban indicators are also estimated by using public information, including the anthropogenic heat.

The methodology was tested in the historic city center of Seville (Spain). The designed mobile transect was repeatedly conducted in July 2019, recording a maximum UHI intensity of 3.1˚C at 22:00 h. A fixed temperature sensor showed that the maximum UHI intensity may be found around 06:00 h, reaching even more than 7˚C. The proposed methodology could be very useful for researchers and policy makers, allowing to direct mitigation strategies and economic investments to areas of particular vulnerability.

Keywords: Urban climate, Urban Heat Island, Microclimate, Mobile transects, GIS.

1 Introduction

1.1 The UHI phenomenon

In the future, it is expected that heat wave events, responsible for many health issues, will be intensified by the Urban Heat Island (UHI) effect (Founda & Santamouris, 2017). The UHI phenomenon is characterized by higher urban temperatures compared to those in the surrounding rural areas. As a result, the UHI effect leads to increased energy needs (cooling energy), environmental issues (formation of smog and air pollutants) and health consequences (such as thermal stress). As a matter of fact, the heat wave that took place in Europe in July 2019 set all-time high temperature records in several countries such as Belgium, Germany, France, the Netherlands or the United Kingdom. The combination of UHI and climate change also leads to a higher air-conditioning demand, which contributes to an increased pressure on electricity generation, transmission and distribution infrastructures (Wang & Akbari, 2016).

One of the Research and Development (R&D) projects trying to reverse the above described situation is the European project CartujaQanat (UIA03-301, CartujaQanat. *Recovering the Street life in a climate changing world*). This project includes the calculation of indicators such as the UHI intensity (UHII), representing the current conditions of urban zones in Seville where climatic control interventions may be potentially applied. In this project, it is proposed to calculate the

variation of the UHII in space and time in a broad area of downtown Seville during the summertime, which led to the present study.

Currently, research studies mainly classify heat islands as either atmospheric (Canopy Layer UHI or Boundary Layer UHI) or surface UHI. Surface UHI refers to the increased warmth of urban surfaces, measured on a large scale by using thermal infrared data from remote sensors in satellites or aircrafts. On the other hand, the Canopy Layer UHI is the one directly related to human exposure, where outdoor thermal comfort is influenced by both air and surface temperatures. The present study will focus on the canopy layer, where the UHII varies in both space and time and shows different patterns depending on the characteristics of the area.

There are many factors that affect the heat island phenomenon, such as the climate characteristics (solar radiation, wind and clouds for instance). In general, it may be said that wind and clouds diminish the heat island effect, whereas clear conditions and calm winds increase it. This is due to the fact that the cloud cover influences the amount of solar energy reaching the earth's surface and the trapping of longwave radiation, and the cloud types (which are related to their height) are also significant (Oke, Mills, Christen, & Voogt, 2017). On the other hand, calm winds reduce the heat that may be convected into the atmosphere, since wind speed is a surrogate measure of atmospheric transport and mixing: the main drivers of advection and turbulent exchange that limit horizontal and vertical temperature differences (Oke et al., 2017). The season and time of day also affect the UHI intensity, as well as the characteristics of the city (ratios of buildings, pavement and vegetation) and the anthropogenic heat release (metabolic heat from humans, traffic, and heat released from buildings). According to the study made by (Santamouris, 2015), who performed an extensive literature review of studies in different locations around the world, the reported UHI intensity varied between 0.4 ˚C and 11 ˚C, with an average of 4.1 ˚C.

For all these reasons, there is a need for a sound scientific background for adaptation and mitigation strategies (Juruš et al., 2016), and also for understanding the physical characteristics of cities to provide eco-system management plans (Liu, Zang, Wang, & Wu, 2018). In addition, achieving accurate climatic characterizations contributes to the theoretical support for climate-conscious eco-city construction (Liu et al., 2017). However, until now UHI mitigation strategies have had negligible contributions to urban development policies and action plans (Parsaee, Joybari, Mirzaei, & Haghighat, 2019).

1.2 Measuring the UHI

The UHI effect may be estimated by using air temperature measurements. The studies that take the field measurement approach define the built environment using geometric features or land use characteristics (Kim, Lee, & Cho, 2017). It is important to consider different locations within the study domain with the purpose of evaluating all its representative areas, and also to carry out the assessment at different times, since the UHI varies during the day. In order to measure air temperatures throughout the city at different times, the optimal option would be to install fixed temperature sensors. However, this is an unfeasible solution due to the high number of sensors that would be needed as well as the intricacies of installing them in public spaces. Therefore, other alternatives should be discussed.

Researchers also face many challenges in the urban environment, since there is a huge scarcity of air temperature data with high spatial resolutions and large spatial coverages. Different methods have been used in the past for measuring the UHI: weather stations in rural environments or airports, fixed weather stations in urban environments, mobile surveys with

ground vehicles, mobile surveys with airborne vehicles or satellite images for surface temperature estimations.

Fixed meteorological stations provide data for long periods with a high accuracy. However, data taken at local airports are not representative of the conditions at the district level, and additional weather stations are expensive, difficult to site and subject to vandalism (Rajkovich & Larsen, 2016). In addition, they would only reflect the climate characteristics of their specific location. Another option could be to consider remote sensing. Due to its wide coverage, open and easy access, researchers began to study the UHIs using this technology (Yao et al., 2018). Nevertheless, even though remote sensing is capable of providing estimates of land surface temperatures in large areas, the information is not so useful to estimate human exposure to air temperature in local areas, since resolution, obstacles such as clouds and cost remain significant limitations. Finer spatial scale data are therefore needed for accurate analyses at the district level and in order to identify key areas of vulnerability (Smith, Webb, Levermore, Lindley, & Beswick, 2011). Whether temporal (mobile surveys) or spatial (weather stations), a compromise is always needed (Azevedo, Chapman, & Muller, 2016).

For these reasons, mobile measurement approaches were proposed as an effective method to analyze temperature distributions within the urban canopy layer, due to the strong influence of local urban parameters. In this way, it is possible to obtain a better understanding of the temperature distributions across urban areas at fine spatial resolutions (Tsin et al., 2016). This method involves mobile surveys with moving equipment, following a route designed beforehand, named “transect”. Mobile transects may present several drawbacks, which will be overcome in the present work:

- Smaller spatial coverage compared to other methods (depending on the length of the designed route).
- The data are only available when the transects are carried out.
- Accurate positional data are needed.
- Lack of simultaneity between the measurements.
- Sensor lags due to high time constants (shown by (Doan, Kusaka, & Nguyen, 2019)).
- Difficulty of designing the transects properly.

However, if designed correctly, mobile transects offer many advantages that will be highlighted in this work:

- High spatial resolution in the area under study.
- High temporal resolution during the measurement period.
- They may be used to locate representative sites for the installation of fixed temperature sensors, or urban planning strategies.
- Low cost compared to other alternatives such as the installation of weather stations.
- They are easy to carry out and different people may be simultaneously involved.

According to the bibliographic review that has been done, most mobile measurements are performed by car or by using bicycles. Cars have the risk of obtaining wrong temperature measurements due to the exhaust gases, and they are not capable of driving all around the city (for example in pedestrian or narrow streets). On the other hand, bicycles are a feasible and low-cost alternative, which is why they present an ideal solution for UHI analyses on a global scale. Those are the reasons why the mobile transects in this work will be carried out by using a bicycle.

1.3 Design of mobile transects

Many studies on the evaluation of the UHI carried out measurements by using mobile transects, but the routes that were followed were chosen in very different ways. Table 1 summarizes the various methods applied for the design of the mobile transects, as described by the reviewed studies. Although most of them followed detailed procedures so as to choose the routes of their mobile transects, the authors of the present work believe that the selection of the optimal transect should not rely solely on driving through areas with different characteristics. As shown by previous sections, the UHI effect depends on many contradictory aspects, which means that designing the route depending only on certain variables could prevent researchers from going through the real representative zones of the area under study. This is the reason why, in the present work, the selection of the optimal mobile transect will rely on experimental measurements instead of relying on data gathered beforehand.

Study	Method
(Rajkovich & Larsen, 2016)	Bicycle paths were selected with a variety of land covers, topographies and paving types, using a random number table to select the path and direction for each ride, and not operating the bicycle at night due to safety concerns.
(Liu et al., 2017)	An effective mobile route was designed by covering most of the typical divided city blocks.
(Sun, Brazel, Chow, Hedquist, & Prashad, 2009)	The route was designed to sample across a typical land cover gradient from urban to rural areas.
(Shi, Lau, Ren, & Ng, 2018)	Two measurement routes were designed to cover a broad range of local climate zones and land cover classes.
(Qiu et al., 2017)	Considered an 8 km long transect with a variety of zones with different vegetation, roads, traffic and buildings.
(Smith et al., 2011)	Determined the route so as to pass through different land use types, following an approximate straight line and passing within a reasonable distance from local weather stations.
(Tsin et al., 2016)	Selected twenty walking routes according to population density, previously estimated air temperatures and average household incomes.
(Dorigon & Amorim, 2019)	Designed two paths east-west and north-south with the purpose of considering a large range of land use and occupation types.
(Yadav & Sharma, 2018)	Their routes were selected intersecting horizontal as well as vertical transects through the city.
(Liu, Liu, & Lin, 2016)	Designed a 17 km long-route to cover the areas of different underlying surface types and various spatial forms for comparative analysis.
(Busato, Lazzarin, & Noro, 2014)	Different paths were fixed in advance crossing urban, sub-urban and rural areas.
(Clay et al., 2016)	A fixed route was selected to ensure that a variety of built conditions were sampled.
(Leconte, Bouyer, Claverie, & Pétrissans, 2015)	Took into account the topography of the conurbation, adapting the itinerary to estimate the influence of topography on the temperature distributions.

Table 1: Methods used to design the mobile transects in the reviewed studies.

1.4 Aim of this study

As seen in the previous literature review, there is a pressing need to figure out the factors that influence the UHI effect in each individual city as well as its temporal and spatial distributions, in order to understand the causal mechanisms and address UHI mitigation through appropriate urban planning policies. For doing so, measurements are the optimal solution. According to (Rajkovich & Larsen, 2016), bicycles are a viable alternative but more work is needed to standardize measurement protocols to allow for comparative studies. Also, according to (Santamouris, 2015) the duration of the reported measurements, season when the monitoring took place, format of the urban heat island intensity and the methodology to select the reference rural station vary considerably between the reported studies, making the comparison between different studies quite difficult. Therefore, the purpose of the present work will be to define a comprehensive methodology for UHI evaluations by carrying out optimal mobile transects, as well as to show how to gather the necessary data that would allow to link the results of the UHI intensity with different urban indicators.

For such a methodology to be useful and replicable, it must rely on public data and affordable solutions. The present work will integrate mobile measurements and spatial interpolations based on Geographic Information Systems (GIS), determining the UHI intensity with a high spatial resolution. In this way, it would be possible to understand how the local climate varies and find areas that are particularly vulnerable. This is done in contrast to previous studies which have traditionally designed the mobile transects based only on land cover types, with the consequent risk of overlooking the most representative areas of the study domain regarding the UHII. In this study, bicycles were chosen as means of transportation due to their flexibility, high spatial resolution as well as the possibility to access all streets (even pedestrian or narrow streets) within the historic center of Seville (Spain), where the methodology has been put in practice. As far as the authors know, this is the first time that mobile transects will be designed by using experimental measurements.

Another important challenge that may be overcome by using the proposed methodology is that it allows to detect the most representative locations in a simple way. Therefore, if a fixed weather station needs to be installed in a certain area, the methodology proposed in this work would allow to place it in the most suitable location, ensuring the representativeness of the measured data.

Since each city around the world is different, a comprehensive methodology such as the one proposed in the present work is needed in order to find solutions that meet the needs of each individual city. By following a highly replicable methodology, the outcomes could be compared for different locations and be used as practical reference for policy makers, allowing to better understand the relationship between the UHI, climate and urban indicators. In this way, it would also be much simpler to propose the appropriate UHI mitigation strategies in each particular location.

2 Methodology

2.1 Outline of the proposed approach

The primary objective of the procedure that will be described in this study is to characterize the outdoor conditions in areas with different climates, urban configurations and characteristics. In order to do so, the first necessary step is to gather information about the study domain. This information will be obtained from public sources, and it would also be necessary as input data for complex or simplified urban simulation models. An example is the one-dimensional model adapted by the University of Seville for the POLIS project (Álvarez Domínguez, 1998), which may be used for predicting air temperature variations within the Urban Canopy Layer (UCL) (Landsberg, 1981; Oke, 1987; Sani, 1990). Apart from gathering information about the study domain, experimental measurements of air temperatures are needed in order to obtain the spatial and temporal UHII distributions.

The methodology of the present study may be divided into the following stages (see Figure 1):

a) First, it is necessary to divide the region into a grid which allows to simplify the reality of all the elements contained within each zone, studying each of them independently.
b) Data of the research domain from different public sources is then gathered, synthesizing the information for each grid cell of the city block division and obtaining urban indicators.
c) In parallel, a fixed temperature sensor is installed in the area under study.
d) A rural weather station is chosen among those available in the surroundings of the study domain, used for the calculation of the UHI intensities.
e) An intensive mobile transect (named supertransect) is carried out, which means to perform a mobile transect that covers as much as possible of the study domain. This will be done only one time.
f) The measurements of the supertransect are evaluated, and spatial interpolation is performed using GIS in order to calculate the average UHII in each grid cell.
g) The previous results of the supertransect allow the design of an optimal mobile transect that covers the most representative areas of the study domain.
h) Once the route is designed, the optimal mobile transect is repeated under different weather conditions, which together with the data from the fixed temperature sensor would allow to obtain the temporal and spatial UHI distribution.
i) Last of all, the temperature measurements during different days together with the data from the rural weather station (including climatic variables such as wind speed, wind direction or solar radiation) as well as the urban indicators of each grid cell would allow the development of very precise UHI correlations that include climate variations.

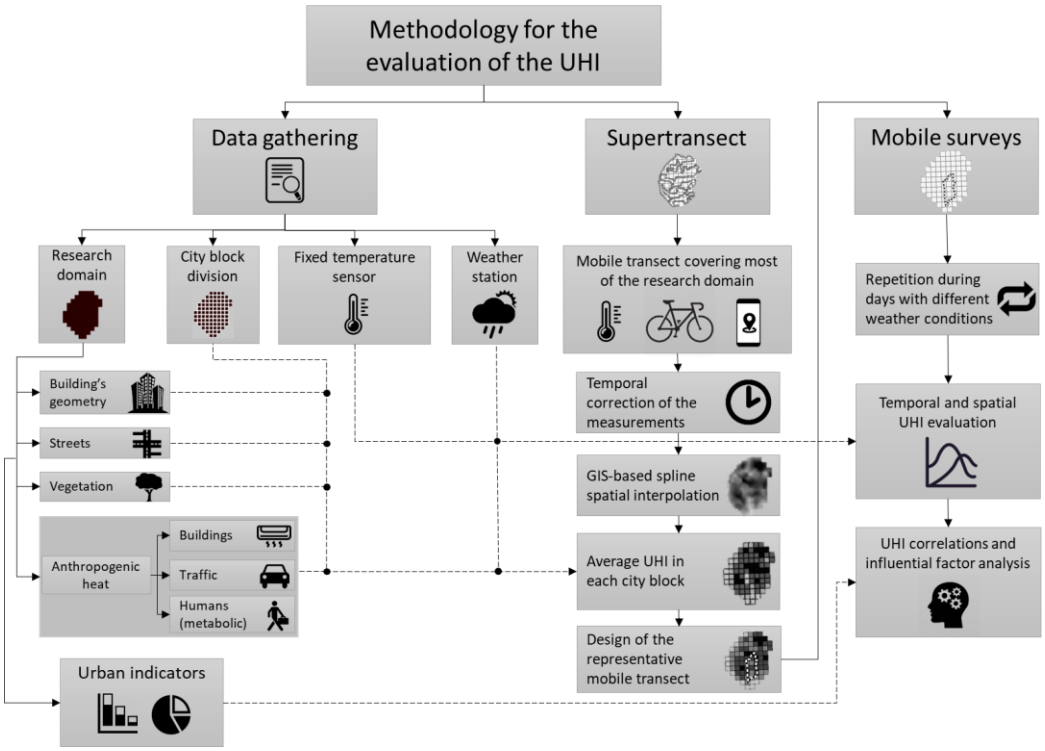

Figure 1: Illustration of the proposed methodology.

2.2 Description of the study area

The present study will be based on the city of Seville, Spain. Due to its geographical location in the southern part of the country, the city has a Mediterranean climate with very high temperatures during summer, reaching over 40 degrees Celsius. Its main feature is the Guadalquivir River, which crosses the city near its historic center and delimits the west boundary of the area under study. In addition, its total population of almost 700,000 inhabitants and high urbanization triggers the well-known phenomenon of the Urban Heat Island, making the outdoor comfort conditions even worse for the people living within the city center. This study is also justified by the fact that Seville is one of the warmest cities in Europe, with a climate classified as Csa (Hot-summer Mediterranean climate) according to the Köppen–Geiger climate classification system. This is the reason why measures against the UHI should be proposed in the area, and the first step to do so would be to evaluate the UHI effect in an accurate way.

2.3 Data acquisition

2.3.1 Instrumentation for the mobile surveys

The methodology proposed in the present work aims to be as much replicable as possible, using common devices that would allow the comparison between studies all around the world. In our case, we decided to perform the mobile transects using a bicycle for several reasons:

- The data are not subject to contamination from vehicle exhaust (which might be the case of cars or motorbikes unless they are electric).
- Its flexibility to drive all around the area under study (even through pedestrian or very narrow streets).
- Very low-cost alternative.

The electric bicycle used for the mobile transects was equipped with two main devices. On the one hand, the air temperatures were measured every 10 seconds (the lowest possible timestep in this case) by using a temperature sensor (resolution: 0.1 °C ; accuracy: ± 0.5 ºC; range: - 40°C to + 85°C; record interval: 10 s to 24 hours). The datalogger was protected by a radiation shield which allowed air to flow around the temperature probe, located at 1.3 meters above the ground. On the other hand, the GPS coordinates were recorded by using an App on a smartphone as shown in the next section, obtaining accurate longitude and latitude data at 1 second intervals. The bicycle maintained a relatively constant speed around 15 km/h to ensure that the measurement points were evenly distributed and sensor lags were avoided. While the bicycle was moving, the sensor responded in less than 10 seconds (the logging interval) to changes in temperature. Several minutes before beginning each session, the air temperature sensor was exposed to outdoor conditions and synchronized with the App.

Figure 2: Equipment used for the mobile transects.

2.3.2 GPS coordinates and GIS software

To ensure the accuracy of the procedure, it is necessary to obtain the exact position of each measurement by using GPS coordinates. In this study, the GPS data were recorded automatically every second by using a smartphone. The widespread availability of smartphones and development of information and communication technologies allow to use a vast amount of data, devices and applications that were not available in the past. If the GPS receiver (which may be assisted by cellular location data) is good enough, smartphones present a very low-cost and accurate alternative for the measurement of GPS coordinates in mobile transects. In this study, two free Apps for obtaining the GPS coordinates were tested: *Geo Tracker* (Android) and *Maps 3D-Outdoor GPS* (IOS). In our case we performed the mobile transects using the latter, although both produced satisfactory results even in the city center of Seville, which is densely built. The example in Figure 3 shows that the Apps that record the GPS coordinates were very accurate, and all the measurements were obtained within the path that was followed. As far as the authors know, this is the first time that the use of smartphones has been reported for obtaining the coordinates in mobile transects.

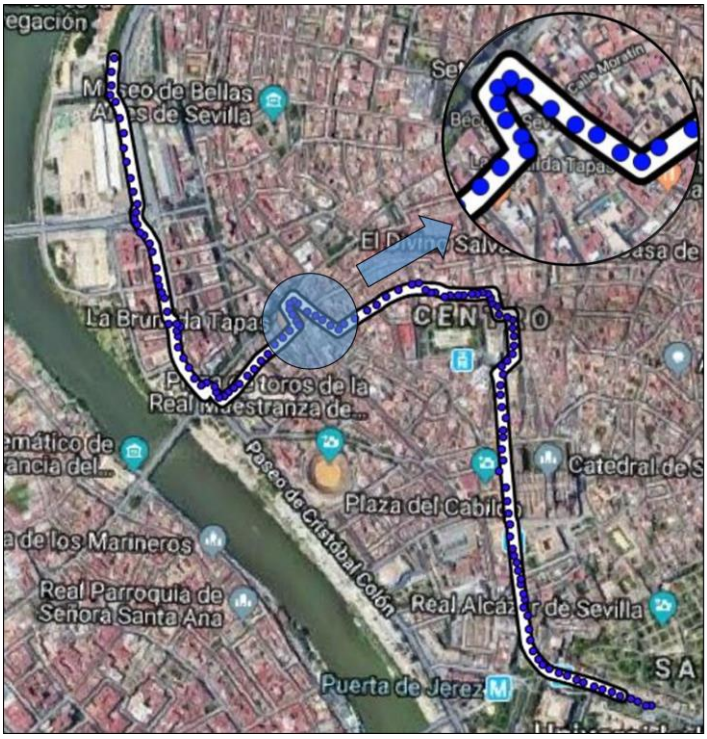

Figure 3: Example of recorded GPS coordinates along a designed route. Background image taken from Google Maps.

On the other hand, Geographic Information Systems are capable of storing geographic objects by using layers of points, lines or polygons. In this study, the software that will be used to handle the GPS coordinates is QGIS (QGIS Development Team, 2016). QGIS (which was previously known as Quantum GIS), is an open-source and free software that supports the analysis of geospatial data, offering endless possibilities such as spatial interpolations, which will be considered in this work. Using the timestamp, the GPS data is linked with the temperature measurements. Then, since each measurement point has associated latitude and longitude data, they may be geolocated using the GIS software, which would then allow to examine and compare the measurements spatially.

2.3.3 Fixed temperature sensor

The temporal distribution of the air temperatures is very important in any UHI study. In order to obtain this information, fixed measurements (which have a low spatial resolution but a very high temporal resolution) are also needed. This would allow to obtain experimental data under different weather conditions, in every season and at different times of the day, and detect when the maximum UHII occurs. Ideally, this information could be available by using weather stations located within the study domain. However, if this were not possible, fixed temperature sensors may be installed as a low-cost alternative, but they should be placed in a representative location. In this work, since it was not possible to obtain data from weather stations deployed within the area under study, a fixed temperature sensor was installed. Its location is shown in Figure 4 and will be validated in the next sections so as to ensure that it was placed in a representative site of the area under study.

2.3.4 Reference weather station

As stated by (Anderson, Gough, & Mohsin, 2018), the proper selection of rural stations is one of the most difficult tasks in UHI analyses. In the case of Seville, there were three nearby weather stations which could potentially be candidates for this study in order to calculate the urban heat

island intensity. Their location may be seen in Figure 4, together with their distance to the centroid of the area under study, highlighted in light blue. These stations provide hourly data about temperature, humidity, wind speed and direction, as well as solar radiation in the case of "La Rinconada" weather station.

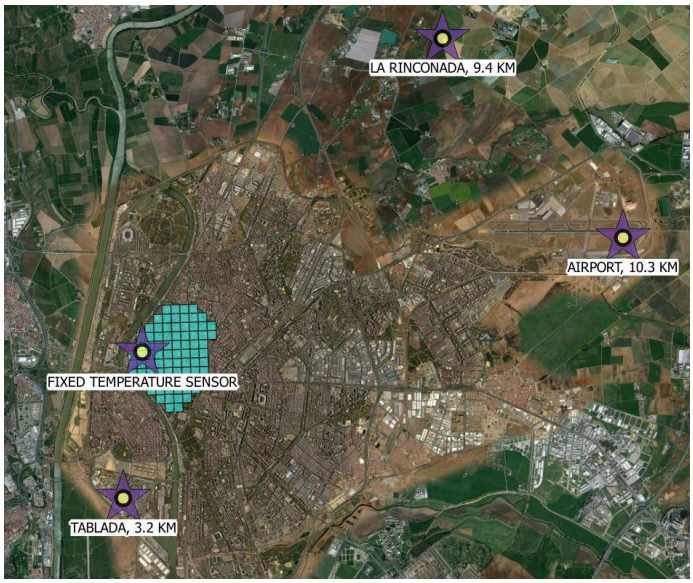

Figure 4: Location of the weather stations and distance to the area under study (shown in light blue).

In order to choose the reference weather station for our study, several issues should be considered. First, we discarded the weather station of "Tablada" due to its proximity to the city. Then, since the other two stations were at a similar distance to the area under study, an analysis of the wind directions and intensity in the area was considered appropriate. In that way, it was possible to estimate which of the stations was more influenced by the higher temperatures in the city. In Figure 5, the wind rose in Seville from the 7th to the 21st of July 2019 (one of the measurement periods) is shown, obtained from ("Wind rose in Seville," 2019). As is apparent, most of the wind is coming from the south-west or the west, which means that the city could influence the temperature of the airport weather station, and the one of "La Rinconada" to a lesser extent. For this reason, we discarded the airport weather station and decided to use the weather station of "La Rinconada" for our study.

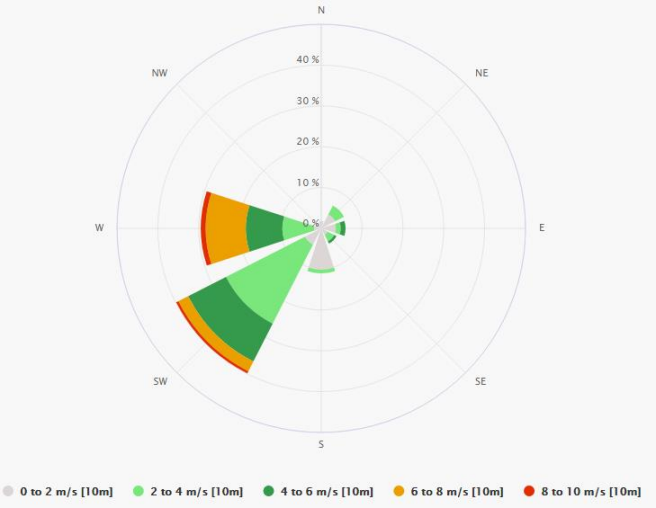

Figure 5: Wind rose in Seville, from the 7th to the 21st of July 2019.

2.4 Index to measure the UHI intensity

To quantify the UHI effect, an appropriate index should be defined first, indicating its intensity. According to many studies, the Urban Heat Island Intensity, known as UHII, should be defined as the difference of temperature between the measurements in the urban area and the temperature of the reference weather station located in a rural area in the surroundings of the study domain, recorded at the same time:

$$UHII = T_{urban} - T_{rural}$$

3 Data gathering

3.1 Partition of the area under study

In order to study the area in detail, first it was divided into different parts. The size chosen for the partitions should be capable of retaining the accuracy of the procedure while considering the differences between the various parts of the city. After consulting other works on the subject (the size considered is similar to that used by other studies such as the one made by (Smith, Lindley, & Levermore, 2009)), the region under study was divided into 82 square grid cells with a spatial resolution of 200 meters (see Figure 6). However, it should be mentioned that the methodology is applicable for other sizes, although data availability should be taken into account. Apart from that, it is also important to know the characteristics of each partition of the study domain: the total area covered by buildings, pavement, vegetation, building height, anthropogenic heat and all the input data that would allow to obtain the urban indicators. The following subsections will explain how to acquire these data.

Figure 6: Grid designed within the study domain.

3.2 Input data obtained from public sources

3.2.1 Buildings

First, data about the buildings in the area under study are needed. Depending on the country, open-access information might be available. In the case of Spain, the geometry of most buildings in the country is available through the Spanish Cadaster, which allows to download in bulk the information of all the building polygons in a city. In addition, the attribute table includes a

parameter with the number of floors of each building. The next step is to extract all the buildings within the case study area. Then, the polygons are filtered to discard those which refer to particular types of buildings (such as underground car parks for instance), and only take into account those above the ground. When that is done, the total height of each building is estimated by assuming a height of 3 meters per floor (which is the typical value in the area under study). In Figure 7, all the buildings within the area under study may be observed, colored depending on their height. As a reference, it should be mentioned that the average building height of the city center is 9.5 meters. In Figure 7, a 3D example is also shown for the buildings that fall within grid cell 35.

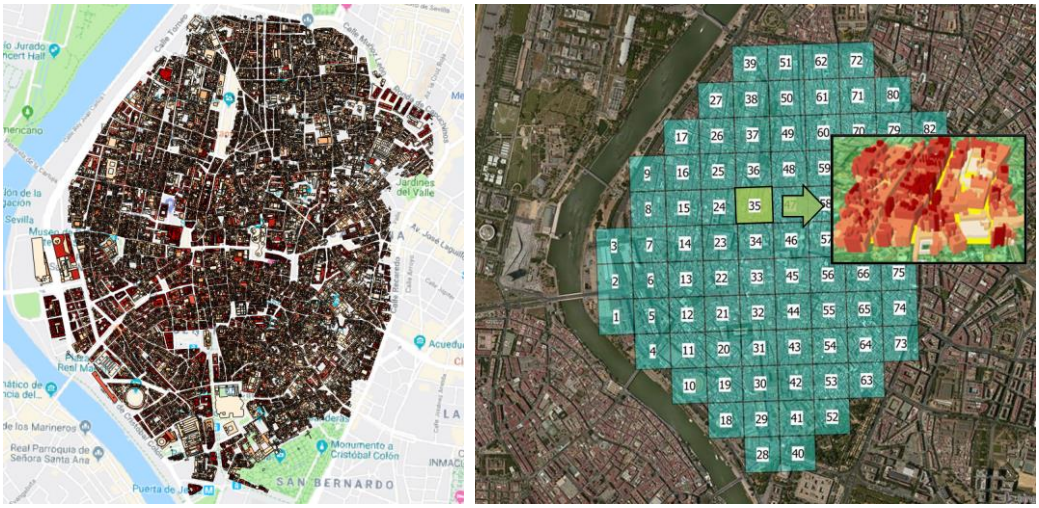

Figure 7: Buildings in the area under study (left) and example of buildings in 3D in the grid cell 35 (right).

In cases where it is difficult to find information about the buildings, it might be useful for researchers to check whether there is open-access information in the free online tool *Overpass turbo* ("Overpass turbo," 2019), which allows to download the information from OpenStreetMap (if available) in different formats. This includes buildings as well as many different elements that may be found in cities, such as water facilities or layers with the streets.

Once all the information about the buildings was available, a GIS software (QGIS) was used to compute the total building area within each grid cell, as well as the average building height. This was done by joining the attributes of the buildings and the grid cells by location.

3.2.2 Streets

Since the geometry of all the buildings and their location is known, it is possible to assume that everything else in the area under study are streets. Obviously, streets include different elements and types of pavement, but knowing the total street area is a necessary first step. Information about the predominant orientation of the streets within each grid cell is also recommendable. This was done by performing a visual inspection of each grid cell.

By making an intersection between the building's layer and the mesh layer and then extracting the inverse area, it is possible to calculate the total street area within each grid cell (see Figure 8). Inner courtyards are included here, since they should not be considered as buildings. The total street area will be then divided into pavement and vegetation.

3.2.3 Vegetation

As just mentioned, within the streets we mainly find either pavement or vegetation. In the case of Seville, open-access information about the trees in the city center is available from the City Council of Seville through its Area of Parks and Gardens. Point layers are available in which it is possible to check the location of all the trees in the city center, as well as to know their species and height. Figure 8 shows all the trees located within the area under study.

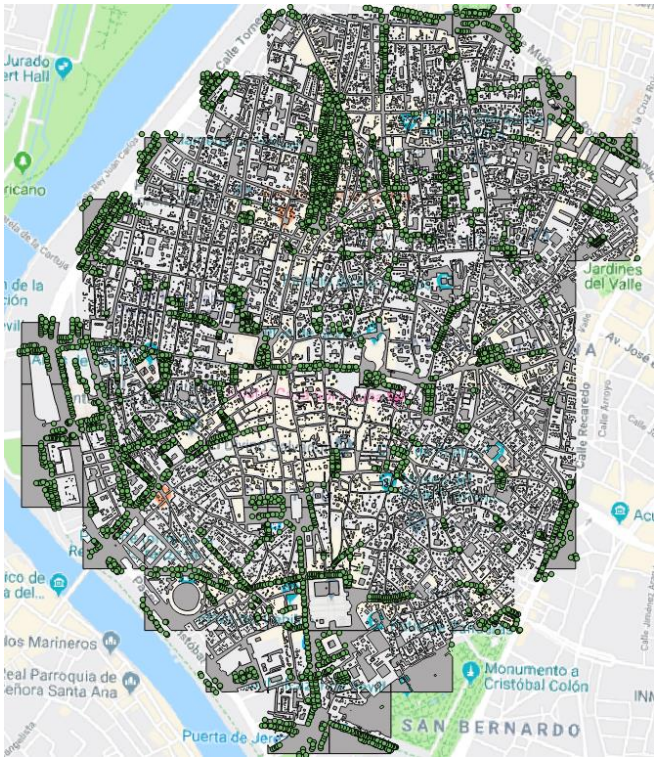

Figure 8 : Polygons of the streets in each grid cell and location of the trees in the case study.

Once the location, species and height of every tree in the area were known, they were categorized into 13 main species. Then, the predominant species in each grid cell was calculated, as well as the average tree height. When the main species of trees in the case study were found, the trees database given in (Forest Ecology and Forest Management Group, 2019) was consulted in order to establish a linear relationship between the treetop diameter and the tree height for each species, using the maximum and minimum values. Together with the predominant species of each grid cell and the average tree height, it was possible to estimate the treetop diameter of every tree.

Following this method, it was possible to estimate the total area covered by vegetation in each grid cell by knowing the total number of trees and assuming a circular shape of each tree when projecting it on the horizontal plane (which depends on the tree diameter). The area covered by vegetation is found within the street area, calculated in the previous section. It will be assumed that the rest of the street area which is not vegetation, is pavement.

3.2.4 Anthropogenic heat

Another important contributor to the UHI effect in any city is the heat released due to human activities, which may be divided into the following types that represent the major sources: metabolic heat produced by the presence of humans, heat generated by traffic and heat emitted by air-conditioning systems in buildings. The anthropogenic heat flux varies widely through the year, through the day and depending on the urban area (Allen, Lindberg, & Grimmond, 2011), and even though typical values range from 5 to 100 W/m^2, even higher values have been reported (Chrysoulakis & Grimmond, 2016).

The anthropogenic heat may be expressed as:

$$Q_{anthropogenic}\left[\frac{W}{m^2}\right] = Q_h + Q_t + Q_b \tag{2}$$

where:

- Q_h is the metabolic heat produced by humans.
- Q_t is the heat generated by traffic.
- Q_b is the heat emitted by the buildings.

An illustration of the distinction considered in this work is shown in Figure 9. This approach is similar to the one followed by other studies. For instance, (Sailor & Lu, 2004) distinguished and developed the same three components separately based on a population density formulation, while (Allen et al., 2011) made the same distinction but developed a model of global anthropogenic heat at 2.5 × 2.5 arc-minute resolution (a much larger scale, about 21 km^2 at the equator). Also, (Smith et al., 2009) considered a bottom-up approach that used readily available data and provided outputs at 200 ×200 m grid square resolution, which is the same as the one chosen for the present study.

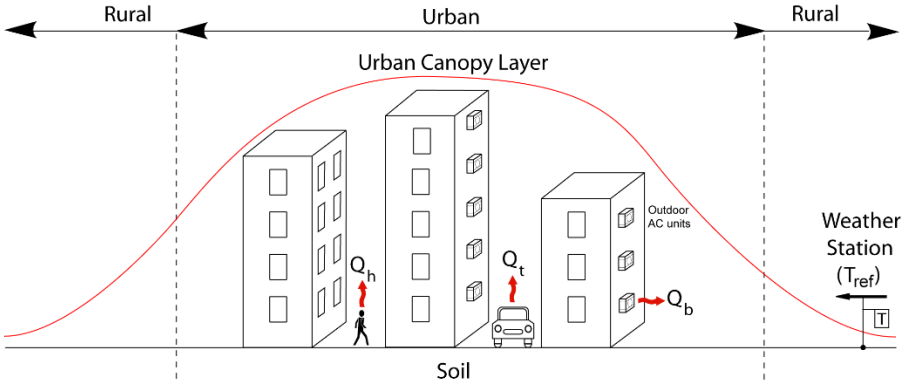

Figure 9: Illustration of the components of the anthropogenic heat.

3.2.4.1 Metabolic heat

The metabolic heat generated by people increases as a function of the physical work performed, and obviously also on the number of people in a certain area. This information is very intricate to quantify, but it may be estimated by using public data. Estimates of Q_h are commonly based upon population statistics (Allen et al., 2011), and may be calculated in the following way for a certain grid cell:

$$Q_h\left[\frac{W}{m^2}\right] = \frac{(N_{inhabitants}+N_{tourists})\cdot M_{rate}}{A_{streets}} \tag{3}$$

where:

- $N_{inhabitants}$ is the number of people living in the area corresponding to the grid cell.
- $N_{tourists}$ is the number of visitors not living in the area.
- M_{rate} is the metabolic rate in [W/person] due to the sensible heat released by people. A value of 71.8 W/person will be considered.
- $A_{streets}$ is the total street area of the grid cell in [m^2].

In the present study, first the people living within each grid cell of the city were estimated by using georeferenced population data, given by the Andalusian Cartography Institute. After linking the information available with the geographical location of each grid cell, the estimation of the inhabitants living in each grid cell of the case study was obtained. Once that was known, people were evenly distributed between the gross surface area of the buildings in the grid cell and the street area. This is due to the fact that the heat gains of the people inside the buildings will be considered in the anthropogenic heat released by buildings, shown in Section 3.2.4.3. Therefore, only the heat gains of the people in the streets were considered here. The results showed a variation of metabolic heat ranging from 0.3 W/m^2 to 1.6 W/m^2 depending on the grid cell.

Apart from the people living in the area, it should be mentioned that Seville is a very tourist-oriented city, with 2,907,754 visitors in 2017 at the historic center of the city ("Sevilla Tourism" 2018). This means that the heat produced by the people visiting the area should be considered. In order to make a rough estimation and due to the lack of more accurate data, the visitors were evenly distributed throughout the year, as well as in the area under study. As a result, tourists and visitors imply an additional 0.17 W/m^2 in each grid cell approximately.

3.2.4.2 Traffic

Determining the contribution of the heat released by traffic is another important issue that should be considered. Even though the city center of Seville has introduced certain traffic restrictions in the recent years in order to protect its historical buildings, it is still a very commercial and touristic area, with traffic of different intensities going through most of its streets. In this study, a similar procedure as the one shown by (Allen et al., 2011) will be followed to estimate traffic heat. This requires data about traffic density, types of vehicles, fuel types and fuel consumption. In this way, the vehicle heat emissions in each grid cell may be calculated as:

$$Q_t\left[\frac{W}{m^2}\right] = \frac{E_{factor} \cdot N_{lanes} \cdot \left(L_{moderate} \cdot D_{moderate} + L_{high} \cdot D_{high}\right)}{A_{streets}} \quad (4)$$

where:

- E_{factor} is the heat emission factor in $\left[\frac{J}{m}\right]$, which depends on the types of vehicles and fuel consumption assumptions.
- N_{lanes} is the average number of lanes of the grid cell.
- $L_{moderate}$ and L_{high} $[m]$ are the total length of streets with moderate and high density of traffic in the grid cell respectively.
- $D_{moderate}$ and D_{high} are the average number of vehicles per hour of each traffic type.
- $A_{streets}$ is the total street area in [m^2].

The following sections will explain how to infer the necessary data.

3.2.4.2.1 Traffic intensity

In order to estimate the contribution of traffic, first it is important to have access to data of all the streets, both their location and length. To do so, data was taken from the open-access online tool *Overpass turbo* ("Overpass turbo," 2019), based on OpenStreetMap. The streets with traffic were located by searching for the word "street", and pedestrian streets were found by searching for "highway=pedestrian". Both layers were exported as a *.kml file, which was later used in QGIS.

On the one hand, pedestrian streets mean that there is no traffic whatsoever. On the other hand, the rest of the streets may have traffic with different intensities. In order to estimate this, it was decided to access the data from Google Maps, which provides information about typical traffic in the main streets at any time of the week. With that information, the streets were categorized in the following way:

a) Pedestrian streets have no traffic.
b) Streets shown in green in Google Maps have moderate traffic.
c) Streets shown in orange or red have a high traffic intensity.

As a result of this categorization, the streets were divided as shown in Figure 10.

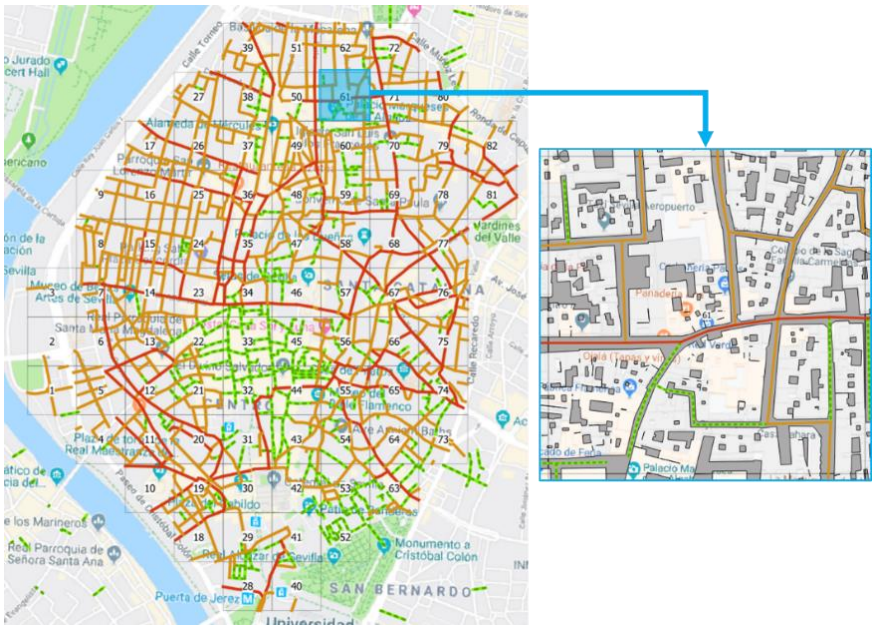

Figure 10: Streets in Seville with no traffic (green), moderate traffic (orange) and high intensity traffic (red).

It is also important to figure out the number of lanes in each street of the area under study. Due to the lack of data in the streets' layers and in order to simplify the process, the average number of lanes in each grid cell was estimated by visual inspection. In this study, most streets had just one lane, although other streets in the area had up to four lanes.

The last step for knowing the heat emitted by traffic, is to figure out the amount of cars going through the streets with moderate or high traffic intensity every hour. To do so, measurements were taken with a digital manual counter in several streets with both types of traffic. As a result, an average value of 132 vehicles per lane and hour was measured for streets with a high traffic intensity, and a value of 72 vehicles per lane and hour was measured for those categorized as moderate traffic. Therefore, considering for instance a street with moderate traffic and 1 lane would mean that 72 vehicles drive along the entire street length during that hour.

3.2.4.2.2 Heat produced by traffic

The heat emission factors of the vehicles driving throughout the city depend on the type of vehicle, type of fuel and fuel consumption rates. Obviously this depends for example on the speed of the vehicles and many other issues, but estimations may be made by following the procedure that is going to be explained, which is similar to that followed by other studies such as the one made by (Smith et al., 2009) or (Sailor & Lu, 2004). We will also assume that the source area for traffic heat emissions is restricted to the streets area.

First, it is important to figure out the fleet of vehicles present in the city. In order to estimate this, open-access data was taken from the National Department of Traffic in Spain, which provides statistics about the fleet of vehicles in every city. In the case of Seville, the categorization shown in Table 2 was made.

Type of vehicle	Percentage of the fleet
Petrol motorbike	10.9%
Petrol car	27.4%
Diesel car	47.4%
Buses	-
Diesel medium size truck	7.5%
Others	6.9%

Table 2: Fleet of vehicles in Seville.

The percentage of buses has been intentionally left in blank in Table 2, since it was estimated in a more accurate way. The City Council of Seville releases a statistical yearbook every year (City council of Seville, 2017), including information about public transport such as the frequency of every bus line. In addition, the public bus company in Seville (Tussam) provides the routes of every bus line. Once the routes and frequency are known, it is possible to infer the total number of buses that drive through each grid cell every hour. Since the total number of vehicles per hour of each grid cell are also known, the percentage of traffic corresponding to buses may be calculated. In this study the percentage varied from 0 % to 78 %, depending on the grid cell. The rest of the percentage is shared for the rest of vehicles according to the estimation shown in Table 2.

The next step is to figure out the heat emission factors for each type of vehicle. In this case, data about mean fuel economy from the study developed by (Zhu, Wong, Guilbert, & Chan, 2017) were taken (shown in the second column of Table 3). The heat emission factor is calculated in the following way:

$$E_{factor} = F_c \cdot \rho_f \cdot NHC_f \cdot \frac{1000}{100000} \quad (5)$$

where:

- E_{factor} is the heat emission factor in [J/m].
- F_c is the fuel consumption in [l/100km].
- ρ_f is the density of the fuel in [kg/l].
- NHC_f is the Net Heat Combustion of the fuel in [kJ/kg].

The results obtained for each type of vehicle are shown in Table 3.

Type of vehicle	Fuel economy [m/l]	Fuel consumption F_c [l/100km]	Fuel density ρ_f [kg/l]	Net Heat Combustion NHC_f [kJ/kg]	Heat emission factor E_{factor} [J/m]
Petrol motorbike	24390.24	4.1	0.75	46400	1427
Petrol car	7800.31	12.8	0.75	46400	4461
Diesel car	9259.26	10.8	0.85	42800	3929
LPG bus	3412.97	29.3	0.58	50200	8531
Diesel medium size truck	3636.36	27.5	0.85	42800	10005
Others	9699.828	10.3	0.76	45720	3563

Table 3: Fuel economy, consumption, density, NHC and resulting heat emission factors for each type of vehicle.

In (Sailor & Lu, 2004), a value of 3,975 J/m was obtained for their average heat emission factor, coherent with the results obtained in the present study. That value was also assumed by other studies such as that published by (Juruš et al., 2016). Finally, in order to calculate the total heat produced by traffic in each grid cell, the equation that was shown in Section 3.2.4.2 should be followed. In this study, Q_t varied from 0 W/m^2 to 12.4 W/m^2.

3.2.4.3 Buildings

The anthropogenic heat release due to different sources in buildings such as lighting, appliances or air-conditioning systems may be estimated in each grid cell by making some assumptions. First of all, it should be mentioned that, in the case of Seville, most of the cooling is provided by using split air conditioning systems whose condensing units are located outdoors (IDAE, Ministry of industry, 2011). Therefore, the released heat should be taken into account due to its influence within the UCL. The study by (Salamanca, Georgescu, Mahalov, Moustaoui, & Wang, 2014) shows that the release of waste heat raises the outdoor temperatures and as a result increases the electricity consumption needed for cooling.

Assuming that buildings are maintained at a relatively constant indoor thermal state, the waste heat generated by hourly electricity consumptions can be thought of as being instantaneously rejected from the buildings (Sailor & Lu, 2004). However, it should be taken into account that most studies neglect the time lag between the consumption of electricity and the measurable waste heat outdoors, since very detailed data of the buildings would be needed (Allen et al., 2011; Boehme, Berger, & Massier, 2015).

In the literature, several procedures have been followed in order to consider the influence of the heat released by buildings. In general, two approaches may be used: bottom-up approaches (which require building-level energy consumption data and therefore big efforts to obtain the information) and top-down approaches (which require annual energy consumption statistics over large areas which are then scaled down both spatially and temporally over the area under study) (Lee, Song, Baik, & Park, 2009). For instance, (Smith et al., 2009) derived building heat emissions by using information about land use, determining the type of buildings within an area, and subsequently the energy use and heat emissions associated with them. In that study, the total heat emissions were also calculated for 200 ×200 m grid cells. Moreover, (Boehme et al., 2015) calculated the gross floor space of buildings and an average electricity load per building, converting it also into an average heat flux density per grid cell. Last of all, (Duan, Luo, Yang, & Li, 2019) presented a lumped urban-building thermal coupling model, comparing the thermal interactions between air-conditioned buildings and naturally-ventilated buildings with their urban environment. Conversely, (Sailor & Lu, 2004) obtained monthly consumption data and

converted it to daily per capita consumption. A similar procedure is followed by (Allen et al., 2011), using the total primary energy consumption statistics of the country to calculate building heat emissions based on population.

Due to its simplicity and the lack of more detailed information, a similar top-down procedure was considered in the present study. In our case, data provided by the City Council of Seville in their statistical yearbook (City council of Seville, 2017) was used, where information about total electricity consumption in the dwellings of the city was provided. Since the total population was known, an estimation of the daily consumption per capita was performed, obtaining an annual average value of 1650 kWh/person in the city. Then, the data obtained in Section 3.2.4.1 about population were used to calculate the total electricity consumption in each grid cell. The values of anthropogenic heat release due to buildings that were obtained (referred to the street area) range between 0.5 W/m^2 and 20.0 W/m^2.

3.3 Summary of input data and discussion

After calculating all the anthropogenic heat contributions of humans, traffic and buildings in each grid cell, it is possible to compare the values that were obtained. As it can be seen in Figure 11, there is a strong variation depending on the grid cell. Some grid cells have a very small contribution of traffic, which is due to the fact that most of its streets are for pedestrians. Also, the contribution of buildings is rather high in most cases. Last of all, it can be seen that the metabolic heat is not negligible due to the more than 50,000 inhabitants living in the area, apart from the tourists visiting the city. As it may be observed, the maximum total value that was obtained is 26.8 W/m^2, and the minimum value is 1.2 W/m^2. The mean value is 13.4 W/m^2. These values are similar to the ones estimated by the studies mentioned in Section 3.2.4.

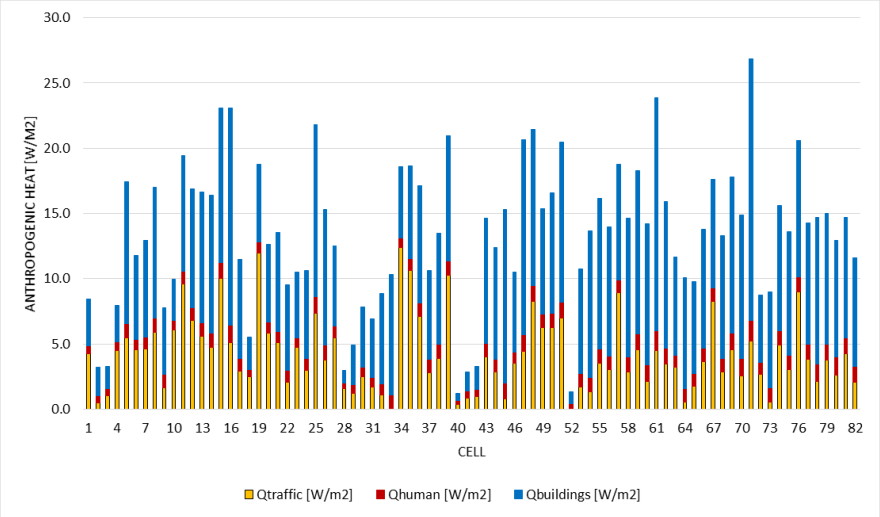

Figure 11: Contributions to the anthropogenic heat in the area under study.

Apart from being influenced by the anthropogenic heat, the microclimatic conditions in the area also depend on the total area covered by buildings, pavement or vegetation. Thanks to the information gathered in Sections 3.2.1 to 3.2.3, it is possible to compute their ratios in each grid cell (see Figure 12). The results show that the area covered by vegetation is the lowest one, although the values strongly depend on the grid cell considered, reaching a maximum of 12%. On the other hand, in the majority of grid cells most of the area is covered by buildings.

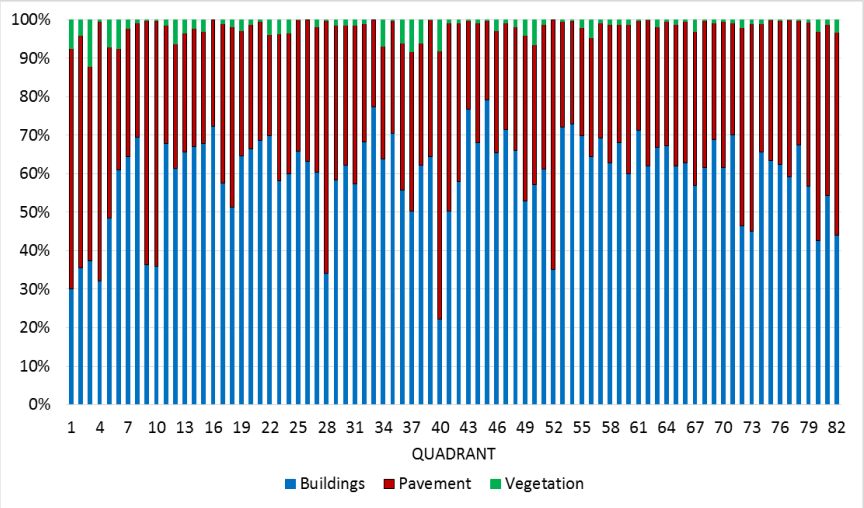

Figure 12: Proportions of buildings, pavement and vegetation in each grid cell.

4 Results of the mobile transects

4.1 Temporal correction of the measurements

In parallel to the data gathering process explained in Section 3, the methodology proposed in the present study (summarized in Figure 1) is based on the design of an optimal mobile transect which may be repeated numerous times in a feasible way. First of all, it should be mentioned that since the temperatures along the mobile transects have non-synchronous observation times, they should be temporally adjusted for comparison purposes. In order to do so, research studies generally use the difference of temperature between the start time and the end time of each transect, generating a linear trend to represent temperature changes during the mobile survey. In this way, it is possible to observe the data obtained from the mobile transect in a synchronous manner.

Different references of temperature are considered depending on the study. For instance, (Liu et al., 2016, 2017; Tsin et al., 2016) used simultaneous data from stationary rural weather stations for the temporal corrections. However, from the point of view of the authors of this study, the mobile transects should begin and end in the same spot so as to be able to compare the temperature difference in the study domain at both times. In this way, there is a more accurate consideration of the real cooling rates in the area, since they are lower in urban areas compared to the rural areas where the weather stations are located. The reference temperature will be the one at the beginning of each mobile transect. Once temporally adjusted, the air temperature data obtained from the mobile transects are compared with the temperatures of the weather station to obtain the UHII, using the timestamp.

4.2 High-resolution mobile transect: supertransect

4.2.1 Characteristics of the supertransect

In the present study, the design of the optimal mobile transect will be based on the measurements taken during one single intensive route, named supertransect. In this way, the proposed route will rely on experimental measurements that allow to capture the numerous interactions in urban areas, as opposed to previous methods that design the routes depending on urban indicators, as shown in the literature review.

The supertransect carried out in this study was designed so as to cover as much as possible of the study domain, taking into account the driving directions for safety reasons. The session began on the 11th of July 2019 at 22:00 h, with a total duration of 1 hour and 49 minutes. The length of the route was 22.04 km, with an average speed of 12.1 km/h. A total of 411 measurement points were taken in 77 of the 82 grid cells into which the study domain was divided. In order to perform the temporal correction explained in Section 4.1, the route began and ended in the same spot. Figure 13 shows the measurements taken during the supertransect once they were temporally corrected, colored depending on their UHII. The results show clear variations within the area under study, with lower temperatures next to green areas, pedestrian streets as well as the river.

4.2.2 Spatial interpolation

To interpret and visualize the UHII measurements with a higher resolution, a spatial interpolation is needed. Spatial interpolation methods are capable of predicting the values of a certain variable at points within the same region of the geolocated source data. This means that it is possible to transform point data to continuous spatial data across the entire research area. In (Yadav & Sharma, 2018), spatial maps of UHII along mobile routes were generated using a kriging interpolation tool. Also, (Liu et al., 2017) used three most commonly used point interpolation approaches: inverse distance weighting, kriging and spline. In the present study, the spline interpolation method has been chosen due to the advantages mentioned by (Liu et al., 2017). Also, (Cui, Yan, Hong, & Ma, 2017) claimed that spline interpolation methods are smoother and give more precisely located extrema, which is why the authors also applied the method. The result of the spatial interpolation in this study is a “heat map”, which provides a visualization of the UHII distribution within the study domain (see Figure 13).

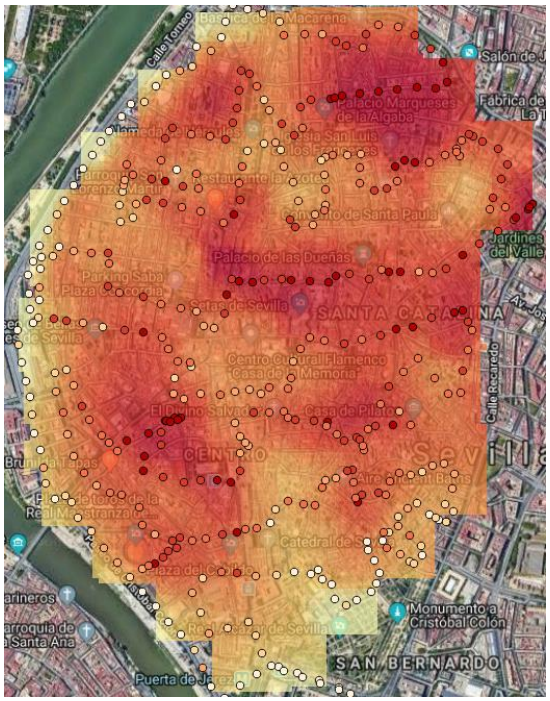

Figure 13: GPS coordinates measured during the supertransect and spatial UHII distribution.

4.3 Design of the optimal mobile transect

Once the spatial interpolation of the measurements taken during the supertransect was performed, it was possible to estimate the UHII in each grid cell by calculating the average of all the values within each of them. In our case, we divided the region into four categories or clusters, depending on the UHII values. The criteria to design the optimal mobile transect may be summarized in the following way:

a) The route should pass through every cluster into which the study domain is divided (4 in our case), preferably in at least two grid cells of each category.
b) The route should not take longer than 20 minutes to perform, so as to ensure its feasibility and replicability during different days or at different times.
c) The driving directions of the streets should be considered for security reasons. Tools such as Google Maps may be used for this purpose.
d) Once designed, the route should be tested once so as to avoid unforeseen circumstances (such as renovation works or changes in street directions).

The optimal route designed in the present study is shown in Figure 14, together with the cluster category of each grid cell (where cluster 1 is the one with the lowest temperatures measured during the supertransect and cluster 4, shown in red, is the one with the highest). Even though there are different possibilities, this route covers all the aspects that were mentioned and maintains an adequate length (3.2 km approximately) to make the route as feasible as possible.

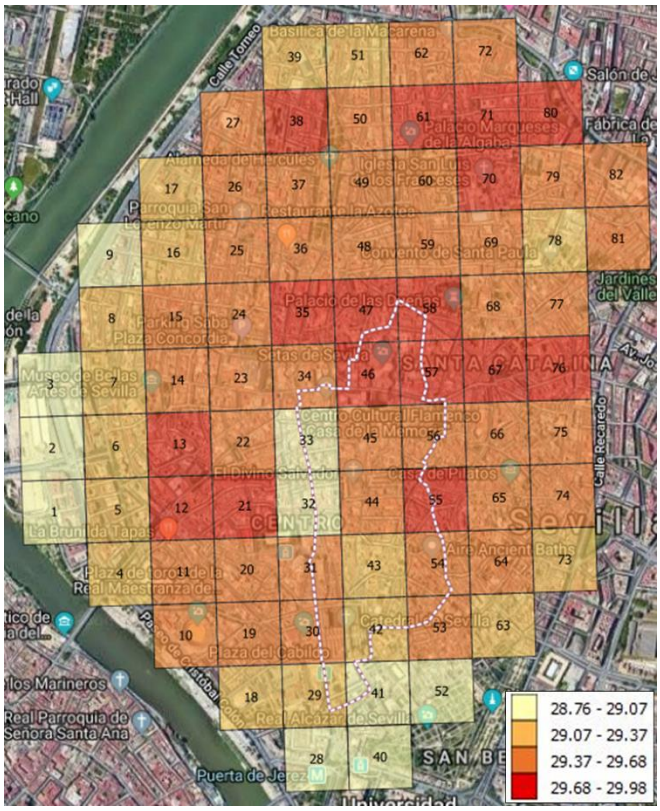

Figure 14: Cluster category of each grid cell and designed optimal mobile transect. The air temperature ranges of each category are shown in the legend in degrees Celsius.

4.4 Validation of the optimal mobile transect

The methodology suggested in the present work aimed to overcome several challenges that are present in any UHI study that considers mobile transects, such as the difficulty of selecting routes that are representative of the area under study. The previous section showed how to design an optimal mobile transect, but experimental data is needed to validate the results obtained when following the proposed methodology. In this way, it would be possible to demonstrate its suitability with regards to the detection of the truly representative locations.

In our case, carrying out the supertransect led to the definition of 4 clusters in the study domain, and eventually the design of the optimal mobile transect. Once the optimal mobile transect has been chosen, it is possible to repeat the route multiple times under different weather conditions, at various times and during different days. To test the proposed methodology, the optimal mobile transect was carried out during 5 days: on the 16th, 18th, 21st, 22nd and 23rd of July 2019. Each day, the optimal mobile transect was done two times: at 09:00 h and at 22:00 h. The measurements were taken at those times so as to measure two very different conditions (after sunrise and after sunset), to minimize the distortion of the measurements due to the effect of solar radiation (although a radiation shield protected the sensor) and also for safety reasons. Each measurement session took around 15 minutes, beginning and ending at the same spot.

In order to validate the suitability of the optimal mobile transect, the measurements obtained at 22:00 h during the 5 days when the methodology was tested were examined. To do so, a box plot was developed (see Figure 15), which shows the upper and lower quartiles as well as the median of the UHII measurements recorded in the grid cells corresponding to each cluster category. Ideally, the small transects and the supertransect should be performed under exactly the same meteorological conditions. In reality, unfortunately this is not possible, so the validation should be performed during days that are as similar as possible. In our case, the small transects and the supertransect were all performed during completely clear days. They also had a very similar total daily solar radiation, and the wind speed was less than 2 m/s in all the cases. As it may be seen, the results validate the designed route since the clusters retain the same tendencies as proposed after conducting the supertransect, with cluster 1 being the one with the lowest temperatures (and therefore UHII) and cluster 4 being the one with the highest measured temperatures.

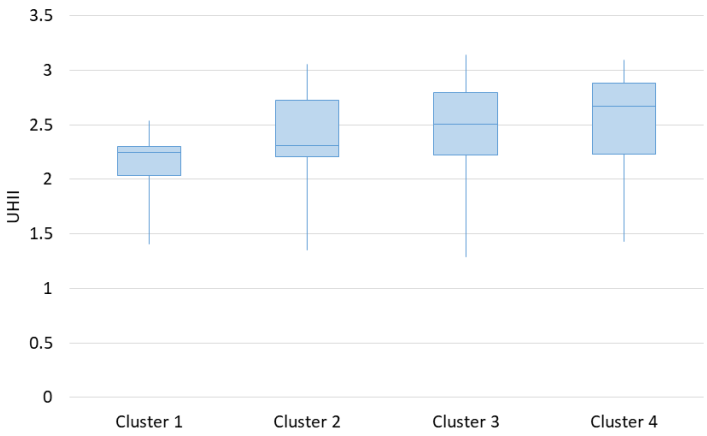

Figure 15: Validation of the supertransect with five days of measurements in the optimal mobile transect.

4.5 Temporal and spatial UHI evaluation

In urban areas, both the UHI spatial and temporal variation are very important. Apart from carrying out the mobile transects, the methodology presented in this work involved also the use of a fixed temperature sensor, whose data would allow to overcome the issue regarding the low temporal resolution of the mobile transects. It may as well be used to extrapolate the measurements or figure out the most critical times when the UHI effect takes place in the study domain. In addition, without a methodology such as the one proposed here it would not be possible to know whether a fixed temperature sensor has been installed in a representative area of the domain under study or not. Therefore, the methodology is also useful to place fixed temperature sensors in an optimal way.

In order to observe the suitability of the location of the fixed temperature sensor that was installed, Figure 16 shows the comparison between the temperature measurements of the fixed sensor and those of the rural weather station. Their difference has been highlighted in blue to observe the UHII temporal variation. In addition, the measurements of the mobile transects are also included (black bars), showing the maximum, minimum and average values (green dots) recorded during each survey. Figure 17 shows the data of the 21st of July in more detail. As is apparent, the fixed temperature sensor was placed correctly, since its measurements (blue line) go through the green dots that show the average temperatures recorded during each mobile transect. This means that it can be considered that the measurements of the temperature sensor are representative of the area under study, demonstrating the relevance of the proposed methodology.

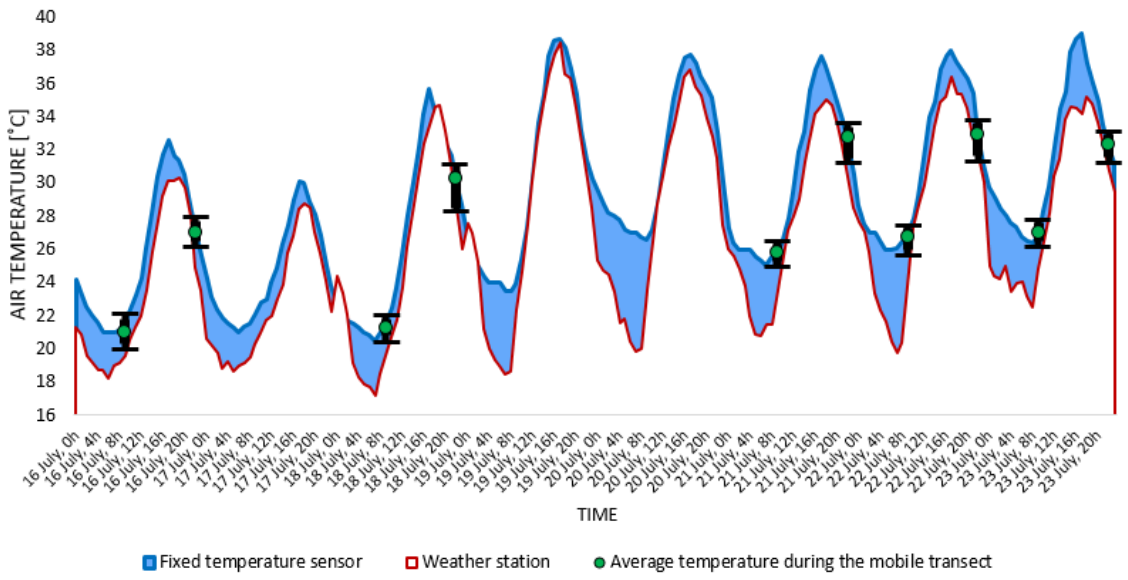

Figure 16: Comparison between the fixed temperature sensor and the weather station during 8 days in July 2019, including the temperatures recorded during the mobile transects.

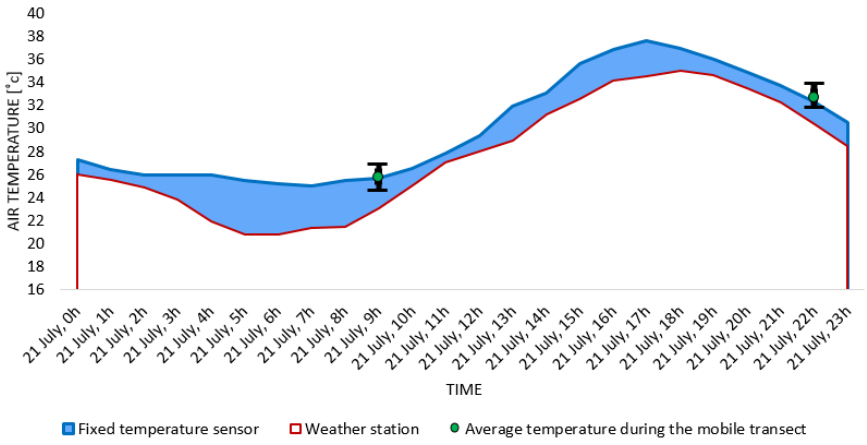

Figure 17: Comparison between the fixed temperature sensor and the weather station during the 21st of July 2019, including the temperatures recorded during the mobile transects.

As it can be seen in Figure 16, the UHII is greater during the night, reaching the highest values around 05:00-07:00 h. The highest observed UHII of the fixed temperature sensor occurred at 07:00 on the 20th of July, reaching a value of 7.18 ˚C. This suggests that areas of the study domain where the UHII is higher than where the fixed temperature sensor is located (its grid cell corresponds to cluster 2) would reach even greater values. Therefore, the highest UHII values were not measured by the mobile transects, neither at 22:00 h nor at 09:00 h. The results reveal that, ideally, the mobile transects should have been carried out around 06:00 h instead, so as to capture the highest UHI intensities. If this were not possible (for security reasons for instance), extrapolation laws could be developed thanks to the installation of the fixed temperature sensor.

5 Conclusions and future work

The aim of the present study was to propose a comprehensive methodology for achieving precise UHI evaluations in urban areas. The method was tested in the city center of Seville (Spain), where public data allowed to estimate the urban indicators of the area under study, which was divided into 82 grid cells. The building area ratios in the grid cells ranged from 22.3% to 79.1%, and the vegetation ratios ranged from 0% to 12%. In addition, the anthropogenic heat was also estimated, obtaining values ranging from 1.2 W/m^2 to 26.8 W/m^2, with an average of 13.4 W/m^2. In parallel, an intensive mobile survey named supertransect was conducted, which allowed to design the route of an optimal mobile transect that covered all the representative UHII categories of the study domain in less than 15 minutes, thus making the method highly replicable. A bicycle was used for the mobile surveys and the GPS coordinates were recorded by using a smartphone, which proved to be a very feasible solution that has never been tested in previous UHI studies as far as the authors know.

Once an optimal route is designed, it may be repeated several times. In this study, the route was tested during five different days, each day at 09:00 h and at 22:00 h. The results showed a maximum UHII value of 3.1˚C, measured at 22:00 h. However, the data obtained from the fixed temperature sensor that was installed in the area under study suggested that the maximum UHII values might be found around 06:00 h. Therefore, a further improvement of the present study would be to perform the mobile transects at times with a higher UHII.

On the other hand, one of the limitations of the proposed methodology is the intrinsic low temporal resolution of the mobile transects: measurements taken during a mobile transect carried out at 22:00 h for instance do not allow to observe the hourly UHII variations that occur during the day. Performing a mobile transect continuously during the same day is not a feasible solution, which is why the present work suggested to install a fixed temperature sensor in a representative area of the study domain. However, a novel alternative that could be explored in the future is the development of hourly air temperature baselines through discrete data obtained from the mobile transects, instead of using a fixed temperature sensor which in turn has a very low spatial resolution.

Future mobile surveys' campaigns should have many replicates of the representative transect so as to have a more accurate representation of the spatial and temporal UHII patterns. Once a sufficient amount of data is gathered, the UHII results of the mobile transects could be linked with the urban indicators and the weather conditions. This could allow to establish precise correlations, identify the most influential variables, develop regression models and eventually calibrate microclimate models for instance.

Studies that are based on experimental measurements and follow a replicable methodology such as the one proposed in the present work, are very important for a proper UHI assessment in any part of the world since they allow to compare different locations, detect areas of vulnerability and suggest possible mitigation measures in an optimal way.

6 References

Allen, L., Lindberg, F., & Grimmond, C. S. B. (2011). Global to city scale urban anthropogenic heat flux: Model and variability. *International Journal of Climatology*, *31*(13), 1990–2005. https://doi.org/10.1002/joc.2210

Álvarez Domínguez, S. (1998). Guidelines on Microclimate Around Buildings. Final Report. POLIS project.

Anderson, C. I., Gough, W. A., & Mohsin, T. (2018). Characterization of the urban heat island at Toronto: Revisiting the choice of rural sites using a measure of day-to-day variation. *Urban Climate*, *25*(November 2017), 187–195. https://doi.org/10.1016/j.uclim.2018.07.002

Azevedo, J. A., Chapman, L., & Muller, C. L. (2016). Quantifying the daytime and night-time urban heat Island in Birmingham, UK: A comparison of satellite derived land surface temperature and high resolution air temperature observations. *Remote Sensing*, *8*(2). https://doi.org/10.3390/rs8020153

Boehme, P., Berger, M., & Massier, T. (2015). Estimating the building based energy consumption as an anthropogenic contribution to urban heat islands. *Sustainable Cities and Society*, *19*, 373–384. https://doi.org/10.1016/j.scs.2015.05.006

Busato, F., Lazzarin, R. M., & Noro, M. (2014). Three years of study of the Urban Heat Island in Padua: Experimental results. *Sustainable Cities and Society*, *10*, 251–258. https://doi.org/10.1016/j.scs.2013.05.001

Chrysoulakis, N., & Grimmond, C. S. B. (2016). Understanding and reducing the anthropogenic heat emission. *Urban Climate Mitigation Techniques*, 27–40. https://doi.org/10.4324/9781315765839

City council of Seville. (2017). Statistical Yearbook Seville. Retrieved from https://www.sevilla.org/servicios/servicio-de-estadistica/datos-estadisticos/anuarios/2017/publicacion/anuario-estadistico-2017.pdf

Clay, R., Guan, H., Wild, N., Bennett, J., Vinodkumar, & Ewenz, C. (2016). Urban Heat Island traverses in the City of Adelaide, South Australia. *Urban Climate*, *17*, 89–101. https://doi.org/10.1016/j.uclim.2016.06.001

Cui, Y., Yan, D., Hong, T., & Ma, J. (2017). Temporal and spatial characteristics of the urban heat island in Beijing and the impact on building design and energy performance. *Energy*, *130*, 286–297. https://doi.org/10.1016/j.energy.2017.04.053

Doan, V. Q., Kusaka, H., & Nguyen, T. M. (2019). Roles of past, present, and future land use and anthropogenic heat release changes on urban heat island effects in Hanoi, Vietnam: Numerical experiments with a regional climate model. *Sustainable Cities and Society*, *47*(November 2018), 101479. https://doi.org/10.1016/j.scs.2019.101479

Dorigon, L. P., & Amorim, M. C. de C. T. (2019). Spatial modeling of an urban Brazilian heat island in a tropical continental climate. *Urban Climate*, *28*(April), 100461. https://doi.org/10.1016/j.uclim.2019.100461

Duan, S., Luo, Z., Yang, X., & Li, Y. (2019). The impact of building operations on urban heat/cool islands under urban densification: A comparison between naturally-ventilated and air-conditioned buildings. *Applied Energy*, *235*(November 2018), 129–138. https://doi.org/10.1016/j.apenergy.2018.10.108

Forest Ecology and Forest Management Group. (2019). Tree Database. Retrieved from https://ajuntament.barcelona.cat/ecologiaurbana/es/servicios/la-ciudad-funciona/mantenimiento-del-espacio-publico/gestion-del-verde-y-biodiversidad/gestion-del-arbolado/buscador-del-arbolado

Founda, D., & Santamouris, M. (2017). Synergies between Urban Heat Island and Heat Waves in Athens (Greece), during an extremely hot summer (2012). *Scientific Reports*, *7*(1), 1–11. https://doi.org/10.1038/s41598-017-11407-6

IDAE, Ministry of industry, trade and tourism. S. government. (2011). SPACHOUSEC Project.

Juruš, P., Resler, J., Derbek, P., Krč, P., Belda, M., Benešová, N., … Hrubeš, P. (2016). High resolution modelling of anthropogenic heat from traffic in urban canopy: A sensitivity study. *2016 Smart Cities Symposium Prague, SCSP 2016*, 1–6. https://doi.org/10.1109/SCSP.2016.7501031

Kim, M., Lee, K., & Cho, G. H. (2017). Temporal and spatial variability of urban heat island by geographical location: A case study of Ulsan, Korea. *Building and Environment*, *126*(October), 471–482. https://doi.org/10.1016/j.buildenv.2017.10.023

Landsberg, H. (1981). The urban climate. *Academic Press, International Geophysics Series*, *28*, 275. https://doi.org/10.1002/joc.3370020312

Leconte, F., Bouyer, J., Claverie, R., & Pétrissans, M. (2015). Using Local Climate Zone scheme for UHI assessment: Evaluation of the method using mobile measurements. *Building and Environment*, *83*, 39–49. https://doi.org/10.1016/j.buildenv.2014.05.005

Lee, S. H., Song, C. K., Baik, J. J., & Park, S. U. (2009). Estimation of anthropogenic heat emission in the Gyeong-In region of Korea. *Theoretical and Applied Climatology*, *96*(3–4), 291–303. https://doi.org/10.1007/s00704-008-0040-6

Liu, L., Liu, J., & Lin, Y. (2016). Spatial-temporal Analysis of the Urban Heat Island of a Subtropical City by Using Mobile Measurement. *Procedia Engineering*, *169*, 55–63. https://doi.org/10.1016/j.proeng.2016.10.007

Liu, Lin, Y., Liu, J., Wang, L., Wang, D., Shui, T., … Wu, Q. (2017). Analysis of local-scale urban heat island characteristics using an integrated method of mobile measurement and GIS-based spatial interpolation. *Building and Environment*, *117*, 191–207. https://doi.org/10.1016/j.buildenv.2017.03.013

Liu, Zang, Z., Wang, W., & Wu, Y. (2018). Spatial-temporal evolution of urban heat Island in Xi'an from 2006 to 2016. *Physics and Chemistry of the Earth*, *110*(November 2018), 185–194. https://doi.org/10.1016/j.pce.2018.11.007

Oke. (1987). Boundary-Layer Climates Second Edition. In *Boundary-Layer Climates Second Edition*. https://doi.org/10.1017/CBO9781107415324.004

Oke, T. R., Mills, G., Christen, A., & Voogt, J. A. (2017). *Urban Climates*. Cambridge University Press.

Overpass turbo. (2019). Retrieved from https://overpass-turbo.eu/

Parsaee, M., Joybari, M. M., Mirzaei, P. A., & Haghighat, F. (2019). Urban heat island, urban climate maps and urban development policies and action plans. *Environmental Technology and Innovation*, *14*, 100341. https://doi.org/10.1016/j.eti.2019.100341

QGIS Development Team. (2016). QGIS Geographic Information System. *Open Source Geospatial Foundation Project*.

Qiu, G. Y., Zou, Z., Li, X., Li, H., Guo, Q., Yan, C., & Tan, S. (2017). Experimental studies on the effects of green space and evapotranspiration on urban heat island in a subtropical megacity in China. *Habitat International*, *68*, 30–42. https://doi.org/10.1016/j.habitatint.2017.07.009

Rajkovich, N. B., & Larsen, L. (2016). A bicycle-based field measurement system for the study of thermal exposure in Cuyahoga county, Ohio, USA. *International Journal of Environmental Research and Public Health*, *13*(2). https://doi.org/10.3390/ijerph13020159

Sailor, D. J., & Lu, L. (2004). A top-down methodology for developing diurnal and seasonal anthropogenic heating profiles for urban areas. *Atmospheric Environment*, *38*(17), 2737–2748. https://doi.org/10.1016/j.atmosenv.2004.01.034

Salamanca, F., Georgescu, M., Mahalov, A., Moustaoui, M., & Wang, M. (2014). Anthropogenic heating of the urban environment due to air conditioning, 1–24. https://doi.org/10.1002/2013JD021225.Received

Sani, S. (1990). Urban climatology in Malaysia: An overview. *Energy and Buildings*. https://doi.org/10.1016/0378-7788(90)90121-X

Santamouris, M. (2015). Analyzing the heat island magnitude and characteristics in one hundred Asian and Australian cities and regions. *Science of the Total Environment*, *512–513*, 582–598. https://doi.org/10.1016/j.scitotenv.2015.01.060

Sevilla Tourism. (2018). Retrieved from https://www.visitasevilla.es/

Shi, Y., Lau, K. K. L., Ren, C., & Ng, E. (2018). Evaluating the local climate zone classification in high-density heterogeneous urban environment using mobile measurement. *Urban Climate*, *25*(November 2017), 167–186. https://doi.org/10.1016/j.uclim.2018.07.001

Smith, C., Lindley, S., & Levermore, G. (2009). Estimating spatial and temporal patterns of urban anthropogenic heat fluxes for UK cities: The case of Manchester. *Theoretical and Applied Climatology*, *98*(1–2), 19–35. https://doi.org/10.1007/s00704-008-0086-5

Smith, Webb, A., Levermore, G. J., Lindley, & Beswick. (2011). Fine-scale spatial temperature patterns across a UK conurbation. *Climatic Change*, *109*(3–4), 269–286. https://doi.org/10.1007/s10584-011-0021-0

Sun, C. Y., Brazel, A. J., Chow, W. T. L., Hedquist, B. C., & Prashad, L. (2009). Desert heat island study in winter by mobile transect and remote sensing techniques. *Theoretical and Applied Climatology*, *98*(3–4), 323–335. https://doi.org/10.1007/s00704-009-0120-2

Tsin, P. K., Knudby, A., Krayenhoff, E. S., Ho, H. C., Brauer, M., & Henderson, S. B. (2016). Microscale mobile monitoring of urban air temperature. *Urban Climate*, *18*, 58–72. https://doi.org/10.1016/j.uclim.2016.10.001

Wang, Y., & Akbari, H. (2016). Analysis of urban heat island phenomenon and mitigation solutions evaluation for Montreal. *Sustainable Cities and Society*, *26*, 438–446. https://doi.org/10.1016/j.scs.2016.04.015

Wind rose in Seville. (2019). Retrieved from https://www.meteoblue.com/es/products/historyplus/windrose/sevilla_españa_2510911

Yadav, N., & Sharma, C. (2018). Spatial variations of intra-city urban heat island in megacity Delhi. *Sustainable Cities and Society*, *37*(November 2017), 298–306. https://doi.org/10.1016/j.scs.2017.11.026

Yao, R., Wang, L., Huang, X., Niu, Y., Chen, Y., & Niu, Z. (2018). The influence of different data and method on estimating the surface urban heat island intensity. *Ecological Indicators*, *89*(September 2017), 45–55. https://doi.org/10.1016/j.ecolind.2018.01.044

Zhu, R., Wong, M. S., Guilbert, É., & Chan, P. W. (2017). Understanding heat patterns produced by vehicular flows in urban areas. *Scientific Reports*, *7*(1), 1–14. https://doi.org/10.1038/s41598-017-15869-6